THE FASEB JOURNAL • RESEARCH • www.fasebj.org

Liver disease–associated keratin 8 and 18 mutations modulate keratin acetylation and methylation

Kwi-Hoon Jang,[*,1] Han-Na Yoon,[*,1] Jongeun Lee,[*] Hayan Yi,[*] Sang-Yoon Park,[†] So-Young Lee,[*] Younglan Lim,[*] Hyoung-Joo Lee,[*] Jin-Won Cho,[*] Young-Ki Paik,[*] Williams S. Hancock,[‡] and Nam-On Ku[*,§,2]

[*]Interdisciplinary Program of Integrated OMICS for Biomedical Science, Graduate School, and [§]Department of Bio-Convergence Integrated Science and Engineering Division, Underwood International College, Yonsei University, Seoul, Korea; [†]Cell Biology and Metabolism Program, Eunice Kennedy Shriver National Institute of Child Health and Human Development, Bethesda, Maryland, USA; and [‡]Barnett Institute and Department of Chemistry and Chemical Biology, Northeastern University, Boston, Massachusetts, USA

ABSTRACT: Keratin 8 (K8) and keratin 18 (K18) are the intermediate filament proteins whose phosphorylation/transamidation associate with their aggregation in Mallory-Denk bodies found in patients with various liver diseases. However, the functions of other post-translational modifications in keratins related to liver diseases have not been fully elucidated. Here, using a site-specific mutation assay combined with nano–liquid chromatography-tandem mass spectrometry, we identified K8-Lys108 and K18-Lys187/426 as acetylation sites, and K8-Arg47 and K18-Arg55 as methylation sites. Keratin mutation (Arg-to-Lys/Ala) at the methylation sites, but not the acetylation sites, led to decreased stability of the keratin protein. We compared keratin acetylation/methylation in liver disease–associated keratin variants. The acetylation of K8 variants increased or decreased to various extents, whereas the methylation of K18-del65-72 and K18-I150V variants increased. Notably, the highly acetylated/methylated K18-I150V variant was less soluble and exhibited unusually prolonged protein stability, which suggests that additional acetylation of highly methylated keratins has a synergistic effect on prolonged stability. Therefore, the different levels of acetylation/methylation of the liver disease–associated variants regulate keratin protein stability. These findings extend our understanding of how disease-associated mutations in keratins modulate keratin acetylation and methylation, which may contribute to disease pathogenesis.—Jang, K.-H., Yoon, H.-N., Lee, J., Yi, H., Park, S.-Y., Lee, S.-Y., Lim, Y., Lee, H.-J., Cho, J.-W., Paik, Y.-K., Hancock, W. S., Ku, N.-O. Liver disease–associated keratin 8 and 18 mutations modulate keratin acetylation and methylation. FASEB J. 33, 9030–9043 (2019). www.fasebj.org

KEY WORDS: intermediate filament · MDB · post-translational modification · protein stability

Intermediate filaments (IFs) are cytoskeletal proteins expressed in a cell-specific and tissue-specific manner, and keratins are the largest subfamily of IFs (1). Keratins are predominantly expressed in simple epithelial cells as specific keratin pairs and are highly differentiated in their expression patterns (2). For instance, a pair of keratin 8 (K8) and keratin 18 (K18) is predominantly expressed in hepatocytes (3). In most cases, mutations in IF proteins predispose or cause a broad range diseases that are associated with tissue-specific expression in different tissue types (4). This reflects their prominent role in cytoprotection from different mechanical and nonmechanical stresses. Mutations in the K8 and K18 pair (K8/K18) predispose their carriers to various liver diseases (5). Thus, through increasing our understanding about human disease–associated keratin mutations, we have also advanced our understanding about the mechanisms of disease development.

Keratins have a tripartite secondary structure composed of a central α-helical rod domain flanked by N-terminal head and C-terminal tail domains (6). Most post-translational modifications (PTMs) in keratins occur in the Ser or Thr residues on the head and tail domains. *In vivo* phosphorylation occurs at K8 Ser24/Ser74 and K18 Ser34/Ser53 on the head domain and at K8 Ser432 on the tail domain, and glycosylation (O-linked N-acetylglucosamine modification) occurs at

ABBREVIATIONS: Ab, antibody; AcK, acetyl-K; ACN, acetonitrile; AdOx, adenosine-2′,3′-dialdehyde; BHK, baby hamster kidney; CHX, cycloheximide; IF, intermediate filament; K8, keratin 8; K18, keratin 18; K8/K18, K8 and K18 pair; LC, liquid chromatography; MDB, Mallory-Denk body; MeR, monomethyl-Arg; MMA, monomethylated Arg; MS/MS, tandem mass spectrometry; PRMT, protein Arg *N*-methyltransferase; PTM, post-translational modification; TSA, trichostatin A; WT, wild type

[1] These authors contributed equally to this work.

[2] Correspondence: Interdisciplinary Program of Integrated OMICS for Biomedical Science, Graduate School, and Department of Bio-Convergence ISED, Underwood International College, Yonsei University, Room 407 Cheamdan Building, 262 Seongsanno, Seodaemun-gu, Seoul 120-749, Korea. E-mail: namonku@yonsei.ac.kr

doi: 10.1096/fj.201800263RR

This article includes supplemental data. Please visit *http://www.fasebj.org* to obtain this information.

0892-6638/19/0033-9030 © FASEB

K18 Ser30/Ser31/Ser49 on the head domain (7–9). Studies using transgenic mice overexpressing keratin PTM mutant proteins demonstrated the critical role of site-specific phosphorylation and glycosylation in hepatoprotection during liver injury (7, 8). These findings were confirmed by the discovery of a natural keratin mutation (K8 Gly62-to-Cys) that inhibits adjacent *in vivo* phosphorylation at K8 Ser74 in patients with liver disease (10).

In addition to phosphorylation and glycosylation, acetylation is involved in the regulation of cellular functions (11). Lys acetylation is catalyzed by Lys acetyltransferases in the ε-amino group of internal Lys residues and neutralizes the positive charge of the amino acids, thus modulating protein functions and cellular processes including gene expression, cell cycle, nuclear transport, receptor signaling, and cytoskeleton reorganizing (12). Regarding cytoskeletal proteins, Lys acetylation occurs in α-tubulin at Lys40, and in actin at Lys61 residues, which enhances the stability of cytoskeletal fibers (13, 14). For K8/K18, Lys acetylation occurs mainly on the rod domain (12), and acetylation at Lys207 in K8 specifically regulates filament organization and solubility (15).

Arg methylation is catalyzed by protein Arg *N*-methyltransferases (PRMTs) that add 1 or 2 methyl groups to a guanidino nitrogen of Arg to produce monomethylated Arg (MMA), symmetrically dimethlylated Arg, and asymmetrically dimethlylated Arg (16). The PRMTs preferentially methylate Arg residues located in Gly and Arg–rich motif and this modification changes positively charged Arg to be more hydrophobic in the nature of the methyl group. Arg methylation results in regulation of several cellular events, such as mRNA splicing, DNA damage repair, cell signaling, protein interaction, and protein translocation (16). Although little is known about Arg methylation of cytoskeletal proteins, biochemical and proteomic studies show that K1, K2a, and K9 are symmetrically dimethlylated (17) and K18 can be methylated at Arg55 (18, 19). However, the validation of methylation sites by site-specific mutagenesis and the functional significance of this modification have not been reported.

Keratin phosphorylation and transamidation are involved in rearranging the keratin cytoskeleton into cytoplasmic inclusions, known as Mallory-Denk bodies (MDBs), found in specific liver diseases such as alcoholic hepatitis and alcoholic cirrhosis (20–22). A recent study using liver biopsy from patients with alcoholic hepatitis showed overexpression of protein kinases, such as spleen tyrosine kinase (SYK) and AKT1 (23). Other studies report that enhanced K8 phosphorylation was observed under several types of stress (24) and increased K8 phosphorylation has been shown to facilitate cross-linking by transglutaminase 2 leading to MDB formation (25). Although the connection between keratin phosphorylation/transamidation and MDB formation has been demonstrated, the effect of human liver disease–associated variants on PTMs remains unknown.

Here, we identified several *in vivo* PTM sites in K8/K18 using nano–liquid chromatography (LC)-tandem mass spectrometry (MS/MS), including phosphorylation at site S13, S34, S258, and S475 and acetylation at K108 in K8, and methylation at R55 and phosphorylation at S401 in K18. We focused on studying keratin acetylation and methylation because those modifications are understudied compared with phosphorylation and glycosylation. The PTMs of acetylation at K108 in K8, methylation at R55 in K18, and methylation at R47 in K8 are reconfirmed by a site-specific mutation. The keratin mutations at the methylation sites caused protein instability, which led to a degradation of the keratins, independent of the ubiquitin-proteasome pathway. However, the mutations at the acetylation sites did not have an effect on protein stability. We compared the acetylation and methylation in liver disease–associated keratin variants, and we found that acetylation of the tested variants, with the exception of K8 G434S, was enhanced; however, methylation of the 2 K18 variants, K18 del65-72 and I150V, was increased in association with stabilization of the variant keratins. These results indicate that the PTMs, specifically methylation, of keratins are involved in regulation of protein stability.

MATERIALS AND METHODS

Cells and reagents

Human colon carcinoma (HT29) and baby hamster kidney 21 (BHK21) cells were obtained from the American Type Culture Collection (Rockville, MD, USA) and grown in Roswell Park Memorial Institute 1640 medium and DMEM, respectively, supplemented with 10% fetal calf serum, 100 U/ml penicillin, and 100 μg/ml streptomycin. Mouse monoclonal antibody (Ab) L2A1, was used for immunoprecipitation of K8/K18 (26). Other reagents used include okadaic acid (OA) (ALX-350-003; Enzo Life Sciences, Farmingdal, NY, USA) and MS-275 (a histone deacetylases inhibitor) (ALX-270-378; Enzo Life Sciences, Farmingdale, NY, USA); trichostatin A (TSA) (T8552; MilliporeSigma, Burmington, MA, USA), nicotinamide (N3376; MilliporeSigma), carbon monoxide–releasing molecule (CORM) (288144; MilliporeSigma), hemin (51280; MilliporeSigma), cycloheximide (CHX) (C1988; MilliporeSigma), adenosine-2′,3′-dialdehyde (AdOx) (A7154; MilliporeSigma), arginine N-methyltransferase inhibitor 1 (AMI-1, a PRMT inhibitor) (A9232; MilliporeSigma), GSK591 (a PRMT5 inhibitor) (SML1751; MilliporeSigma), MS049 (a PRMT4/6 inhibitor) (SML1553; MilliporeSigma), and chymo trypsin (MilliporeSigma); trypsin (Promega, Madison, WI, USA); and proteasome inhibitor *N*-acetyl-Leu-Leu-norleucinal (ALLN) (208719; MilliporeSigma). The following antibodies were used: anti-K8 (TS1) (MA5-14428; Thermo Fisher Scientific, Waltham, MA, USA), anti-K18 (DC10) (MA1-12589; Thermo Fisher Scientific), anti-acetyl-K (AcK) (9441; Cell Signaling Technology, Danvers, MA, USA), anti-monomethyl-Arg (MeR) (Ab414; Abcam, Cambridge, MA, USA), anti-di-MeR, symmetric (SYM10) (07-412; MilliporeSigma) and anti-di-MeR, asymmetric (ASYM24) (07-414; MilliporeSigma), anti-Symmetric Di-Methyl Arg Motif Mutimap (sdme-RG) (13222; Cell Signaling Technology), anti-Asymmetric Di-Methyl Arg Motif Multimap (adme-R) (13522; Cell Signaling Technology), anti-pan actin (MA5-11869; Thermo Fisher Scientific), anti-α-tubulin (T5168; MilliporeSigma), and HA-probe (sc-805; Santa Cruz Biotechnology, Dallas, TX, USA). The following antibodies directed to keratins were previously described (26): anti-K8/K18 (8592), anti-K8 phosphorylation at S74 (LJ4), anti-K8 phosphorylation at S432 (5B3), and anti-K18 phosphorylation at S53 (3055).

Cell culture and treatment

HT29 cells were treated with either *1*) okadaic acid (1 μg/ml, 2 h) (24) to enhance the accumulation of phosphorylated keratins, *2*) TSA/MS-275/nicotinamide (2 μM/5 μM/20 mM, 24 h) (12, 27) to enhance the accumulation of acetylated keratins, or *3*) CORM/hemin (100/10 μM, 10 h) (28) to enhance the accumulation of methylated keratins. Cells were solubilized with 1% Igepal CA630 (CA-630) (I8896; MilliporeSigma) or 0.5% Empigen BB (Emp) (30326; MilliporeSigma) in PBS containing 5 mM EDTA, 0.1 mM PMSF, 25 μg/ml aprotinin, 10 μM leupeptin, and 10 μM pepstatin (26). Then, samples were incubated with either anti-K8/K18 (L2A1), anti-AcK, or anti-MeR Ab or the samples were extracted within high salt condition, as previously described (26). Immunoprecipitates or high salt extracted samples were analyzed by SDS-PAGE followed by Coomassie blue staining or immunoblotting with antibodies. For analysis of protein stability, BHK21 cells were transfected with keratin constructs and treated with CHX (100 μg/ml) for 12, 36, or 60 h. Total cell lysates were prepared and analyzed by SDS-PAGE followed by immunoblotting with anti-K8/K18 antibodies or anti-actin Ab.

To examine the effect of methylation inhibitors, the transfected BHK21 cells were treated with 20 μM AdOx (29–31), a global mehthyltransferase inhibitor; 100 μM AMI-1 (29, 32), a PRMT inhibitor; 5 μM MS049 (33), a PRMT4/6 inhibitor; or 5 μM GSK591 (30), a PRMT5 inhibitor (for 48 h). The K8/K18 immunoprecipitates were prepared and then immunoblotted with anti-MeR Ab. To compare the filament assembly after treatment with the methylation inhibitor, the transfected cells were treated with DMSO or AdOx (20 μM) for 24 or 48 h, then stained with anti-K8/K18 Ab (8592) and DAPI. Images were obtained using a Zeiss Axio Imager Z2 (Carl Zeiss, Oberkochen, Germany).

In gel digestion

K8 and K18 bands were excised from SDS-PAGE gel and then destained with washing solution [25 mM NH4HCO3 with 50% acetonitrile (ACN)]. After dehydration in 100% ACN, the gel pieces were dried in a SpeedVac. The samples were incubated with trypsin (0.025 μg/μl) or chymotrypsin (0.025 μg/μl) for 18 h at 37°C. Digested peptides were extracted with 50% ACN twice and dried in a SpeedVac.

Mass spectrometric analysis of K8/K18 peptides

For phosphorylation, peptides were separated within a nano-LC instrument (LC-Packings) as the solvent and had been changed with the flow rate of 200 nl/min. Solution A (0.1% formic acid with 5% ACN) was first used for 15 min to remove salts. During the next 1 h, the ratio of solution A to solution B (0.1% formic acid with 90% ACN) had gradually changed to 68:32. For the last 19 min, the solution gradually changed and substituted to solution B entirely. After ionization from nano-electrospray ion sources (Protana, Odense, Denmark), peptides were analyzed *via* QSTAR Pulsar (Thermo Fisher Scientific) using collision-induced dissociation with nitrogen. Peptide spectrum data were acquired using the Information-Dependent Acquisition mode with a range of 400–1500 *m/z* data at an interval of 3 s. For acetylation assay, peptides were separated within an Easy *n*-LC (Thermo Fisher Scientific). The capillary column (150 × 0.075 mm) was obtained from Proxeon (Odense, Denmark), and the slurry was packed in-house with a 5 μm, 100 A pore size Magic C18 stationary phase resin (Michrom BioResources, Auburn, CA, USA). The mobile phase C for LC separation was 0.1% formic acid in deionized water, and the mobile phase D was 0.1% formic acid in ACN. Chromatography gradient was designed for a linear increase from 5% B to 35% B in 30 min, 40% B to 60% B in 5 min, 90% B in 10 min, and 5% B in 15 min. Flow rate was maintained at 300 nl/min. Linear Trap Quadrupole-Orbitrap MS (Thermo Fisher Scientific) was used for peptide identification. Mass spectra were acquired using data-dependent acquisition with a full mass scan (350–1200 *m/z*) followed by 5 MS/MS scans. For MS1 full scans, the orbitrap resolution was 30,000 and the automatic gain control (AGC) was 2×10^5. For MS/MS in the Linear Trap Quadrupole, the AGC was set as 1×10^4. For methylation assay, peptides were separated in a nano-HPLC system (Agilent Technologies, Santa Clara, CA, USA) using a nanochip column (150 × 0.075 mm). Mobile phases C and D were used. Product ion spectra were collected in the Information-Dependent Acquisition mode and were analyzed by Agilent 6530 Accurate-Mass Q-Time of Flight (TOF) (Agilent Technologies) using continuous cycles of 1 full scan TOF MS from 350 to 1500 m/z (3 spetra/1 s) plus 3 product ion scans from 100 to 1700 m/z (1 spectra/1 s). Precursor m/z values were selected (starting with the most intense ion) using a selection quadrupole resolution of 3 Da. The dynamic exclusion time for precursor ion m/z values was 60 s.

Database search

Acquired MS/MS data were analyzed using the Mascot search engine (*http://www.matrixscience.com*) (Matrix Science, London, United Kingdom), whereby the search parameters for PTM sites were set using the taxonomy of *Homo sapiens* within the SwissProt (*https://www.uniprot.org/uniprot/?query=reviewed:yes*) database. For phosphorylation (QSTAR Pulsar), the enzyme was accepted as trypsin or chymotrypsin, allowing cleavage missing up to 1, oxidation at methionine and phosphorylation at Ser/Thr/Tyr as variable modifications, and 2+ and 3+ peptide charges; 1.2 Da was set for peptide tolerance, and 0.6 Da was set for MS/MS tolerance. For acetylation (Orbitrap), the enzyme was accepted as trypsin, allowing cleavage missing up to 1 and variable modification, oxidation at methionine, acetylation at Lys residue, and maximum allowed missed cleavage; 2, MS tolerance; 10 ppm, MS/MS tolerance; 0.8 Da. Peptides were filtered with a significance threshold of $P < 0.05$. For methylation (6530 Accurate-Mass Q-TOF), mass tolerances of 100 ppm and 0.1 Da were used for precursor and fragment ions, respectively. Peptides were oxidized at methionine residues and methylated at Lys or Arg. Post-translational modified peptides expected by Mascot were inspected manually, and the modification sites were compared in the PhosphoSitePlus (*http://www.phosphosite.org*).

Statistical analysis

Densitometry was conducted using ImageJ software (National Institutes of Health, Bethesda, MD, USA), and the graph data were presented as the means ± SD. Statistical analysis was conducted using Student's t test from the 3 independent experiments. A value of $P < 0.05$ was considered as significant.

RESULTS

Identification of PTM sites in K8/K18 by nano-LC-MS/MS

The HT29 cells were treated with okadaic acid (an inhibitor of protein phosphatase-1 and -2A) (34), a combination of TSA, MS-275, and nicotinamide (inhibitors

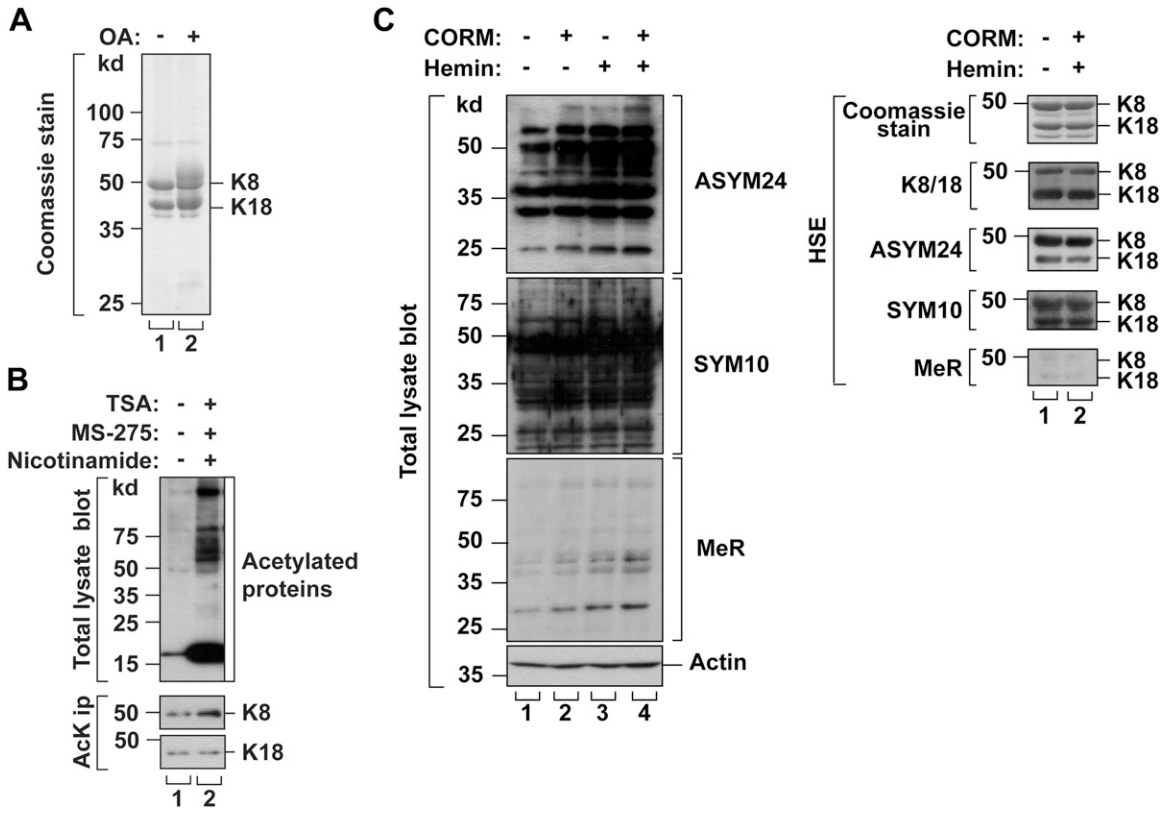

Figure 1. Verification of PTMs of K8 and K18 *in vivo* after okadaic acid (OA), TSA/MS-275/nicotinamide, or CORM/hemin treatment. *A*) HT29 cells were treated with phosphatase inhibitor (OA; 1 μg/ml, 2 h). K8/K18 were immunoprecipitated using L2A1 Ab. K8/K18 immunoprecipitates were analyzed by SDS-PAGE, followed by Coomassie Blue staining. Hyperphosphorylated keratins were detected as blurred bands just above the major K8 or K18 bands. *B*) HT29 cells were treated with deacetylase inhibitors (TSA/MS-275/nicotinamide; 2 μM, 5 μM, and 20 mM for 24 h). Acetylated proteins were immunoprecipitated with anti-AcK Ab and separated by SDS-PAGE followed by immunoblotting with anti-K8 or K18 Ab. The level of K8 acetylation was enhanced after inhibitor treatment, whereas the level of K18 acetylation was similar to that of basal conditions. *C*) HT29 cells were incubated with enhancers of Arg methylation (CORM/hemin; 100 and 10 μM for 10 h). Using anti-mono-MeR antibody, anti-symmetric di-methylated Arg antibody (SYM10) and anti-asymmetric di-methylated Arg antibody (ASYM24), both methylome and methylated keratins were confirmed from total lysate and high salt extracted fraction, respectively. Actin blot for total lysates and Coomassie staining for high salt extracted were used as loading control. HSE, high salt extracted.

of deacetylases) (12, 27), or a CORM with hemin (enhancers of Arg methylation) (28) to enhance the accumulation of phosphorylated, acetylated, or methylated K8/K18 proteins, respectively. Phosphorylation and acetylation on the keratins were confirmed by detection of slower migrated phosphorylated keratins (**Fig. 1*A***) or by using anti-AcK Ab (Fig. 1*B*). Methylated proteins in high salt extracted samples whose positions were overlapped with K8 and K18 were detected by using anti-methylated Arg antibodies (Fig. 1*C*). To identify the specific PTM sites, we prepared immunoprecipitated K8/K18 from the cells treated with specific PTM enhancer(s), and the immunoprecipitated keratins were digested with trypsin or chymotrypsin followed by nano-LC-MS/MS. The results are summarized in **Table 1**. The identified PTM sites were phosphorylated Ser13/Ser21/Ser24/Ser34/Ser258/Ser475 in K8 and Ser34/Ser53/Ser401 in K18, acetylated Lys108 in K8 and Lys187/Lys426 in K18, and monomethylated Arg55 in K18 (Supplemental Figs. S1 and S2 and Table 1). The identified acetylation and methylation sites were highly conserved in other IF proteins (Supplemental Table S1).

Verification of acetylated Lys and monomethylated Arg sites in K8 and K18 by mutagenic approach

Because the significance of keratin acetylation/methylation in cellular events has not been well studied, we focused on further examining these PTMs. Previous proteomic studies indicated the multiple potential acetylation/methylation sites of K8 and K18 (12, 14, 18, 19). However, with the exception of acetylated Lys207 in K8 (15), most of the potential keratin PTM sites that were identified by high throughput analysis have not been validated biochemically such as using site-directed mutagenesis. We generated Lys-to-Arg mutants at K8 and K18 acetylation sites and Arg-to-Lys/Ala at the methylation sites, and BHK cells were cotransfected with a combination of K8/K18 wild type (WT) or mutants. K8 and K18 were cotransfected because they form obligate heteropolymers (35). Acetylated proteins were immunoprecipitated with anti-AcK Ab, followed by immunoblotting with K8/K18 antibodies or tubulin Ab (as a control of known acetylated protein). Acetylation of mutant keratins, particularly K8 K108R, was dramatically reduced

TABLE 1. *PTM sites on K8 and K18*

PTM[a]	Protein	Protease	Observed *m/z*	Charge state (+)	M_r(expt)	M_r (calc)	Δ	Peptide sequence	PTM site	Ions score[b]	Number of records in the website[c]	
											LTP	HTP
P	K8	Trypsin	581.2730	2	1160.5315	1160.5227	0.0088	^{9}SYKVpSTSGPR^{18}	S13	58	1	10
			770.3416	2	1538.6687	1538.6515	0.0172	^{19}AFSSRpSYTSGPGSR^{32}	S24	46	5	122
			921.8929	2	1841.7713	1841.7945	−0.0232	^{24}SYTSGPGSRIpSSSSFSR^{40}	S34	52	1	56
			1231.0723	2	2460.1300	2460.1243	0.0056	^{253}SLDMDpSIIAEVKAQYEDIANR^{273}	S258	85	0	22
			777.3807	2	1552.7468	1552.7386	0.0082	^{470}DGKLVpSESSDVLPK^{483}	S475	53	0	31
		Chymo-	855.3720	2	1708.7294	1708.7934	−0.0639	^{11}KVSTSGPRAFpSSRSY^{25}	S21	31	0	49
		trypsin	965.3941	2	1928.7737	1928.8265	−0.0529	^{21}SSRpSYTSGPGSRISSSSF^{38}	S24	59	5	122
	K18	Trypsin	978.7836	3	2933.3289	2933.3669	−0.0380	^{15}SLGSVQAPSYGARPVSSAApSVYAGAGGSGSR^{45}	S34	42	14	36
			992.7705	3	2975.2897	2975.3219	−0.0323	^{382}RLLEDGEDFNLGDALDSSNpSMQTIQK^{407}	S401	91	0	11
			940.7355	3	2819.1848	2819.2208	−0.0360	^{383}LLEDGEDFNLGDALDSSNpSMQTIQK^{407}	S401	79	0	11
		Chymo-	622.7812	2	1243.5479	1243.5598	−0.0119	^{25}GARPVSSAApSVY^{36}	S34	59	14	36
		trypsin	882.3827	2	1762.7509	1762.7999	−0.0491	^{37}AGAGGSGSRISVSRSTpSF^{54}	S53	40	16	25
A	K8	Trypsin	562.8082	2	1123.6019	1123.6026	−0.0006	^{102}FASFIDaKVR^{110}	K108	28	0	7
	K18	Trypsin	608.8300	2	1215.6454	1215.6459	−0.00044	^{187}aKVIDDTNITR^{196}	K187	41	1	3
			608.8302	2	1215.6458	1215.6459	−0.00005	^{187}aKVIDDTNITR^{196}	K187	28	1	3
			701.8809	2	1401.7472	1401.7464	0.00058	^{418}VVSETNDTaKVLR^{429}	K426	26	0	4
			701.8803	2	1401.7459	1401.7464	−0.00029	^{418}VVSETNDTaKVLR^{429}	K426	30	0	4
M	K18	Trypsin	951.8030	3	2852.3871	2852.3907	−0.0036	^{51}STSFmRGGMGSGGLATGIAGGLAGMGGIQNEK^{81}	R55	114	0	16
			951.8053	3	2852.3941	2852.3907	0.0033	^{51}STSFmRGGMGSGGLATGIAGGLAGMGGIQNEK^{81}	R55	97	0	16

Mass spectrometric analysis and database search were described in Materials and Methods. Briefly, K8 and K18 bands were excised and digested with trypsin or chymotrypsin, respectively. The PTM sites were verified by manual inspection of LC-MS/MS spectra showing mass shift of b- and y-ion series from unmodified peptide mass (phosphorylation, +80 or −98 Da (neutral loss); acetylation, +42 Da; methylation, +14 Da). LC-MS/MS spectra with Mascot score >20 were chosen and presented in this table as feasible PTM peptides. [a]A, acetylation; M, methylation; P, phosphorylation. [b]Ions score: probability based on molecular weight search (MOWSE) score ($P < 0.05$). [c]Based on data in the website (*www.phosphosite.org*), all PTM sites of K8 and K18 in this study have been reported in low throughput papers (LTPs) or high throughput papers (HTPs), or both. Note that the number of LTPs in which the modification site was determined using methods other than discovery MS, and the number of HTPs was assigned using only proteomic discovery MS.

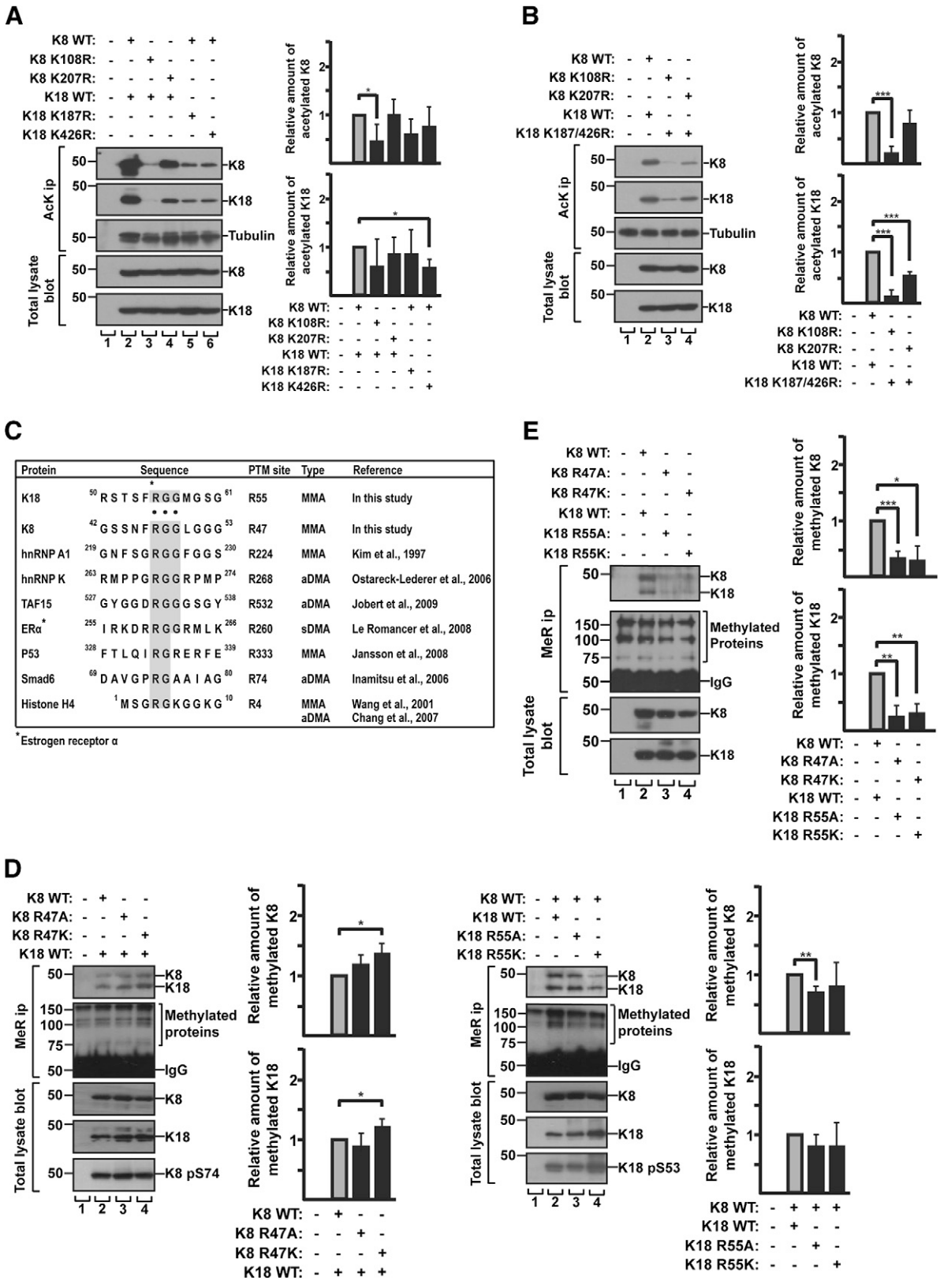

Figure 2. Identification of acetylation/methylation sites of K8 and K18 using acetylation and methylation mutant keratins. *A*) BHK cells were cotransfected with K18 WT and K8 acetylation mutant construct (Lys-to-Arg mutant; K108R or K207R), or with K8 WT and K18 acetylation mutant construct (K187R or K426R). Cells were treated with TSA/MS-275/nicotinamide and harvested after 24 h. Levels of acetylated K8 and K18 were verified by immunoprecipitation using anti-AcK Ab, followed by immunoblotting with anti-K8 and anti-K18 antibodies. Tubulin blot was used as a loading control. *B*) K8 K108R or K8 K207R together with K18 K187/426R were transfected in BHK cells. Transfected cells were analyzed as described in *A*. The graph represents means ± SD of 3 independent experiments. *C*) Comparison of the sequence adjacent to methylation motif (RGG; Arg-Gly-Gly) site of keratins

(*continued on next page*)

(**Fig. 2*A***). These findings indicate that Lys108 was a major acetylation site, along with Lys207, a previously characterized site. To minimize the effect of acetylated Lys in counterpart keratin WT on binding with anti-AcK Ab, each K8 mutant (K108R or K207R) was cotransfected with K18 double mutant (K187/426R) and the acetylation level of mutants were compared with the levels of K8 and K18 WT. Cotransfection of K18 K187/426R with K8 K108R showed a notable reduction of acetylated keratins, and to a lesser extent, the same was evident in K8 K207R (Fig. 2*B*). Both results showed that Lys108 in K8 was one of the major acetylation sites. Similar to K207R, the K8 K108R mutation resulted in about 20–30% reduced phosphorylation at K8 Ser74 as compared with the phosphorylation of K8 WT, whereas the level of phosphorylation at K8 Ser432 was similar in both K8 WT and acetylation mutants (Supplemental Fig. S3).

Our mass spectrometry analysis showed monomethylation at K18 Arg55 (RSTSF^{55}RGGMGSG) (Table 1) located in the Gly and Arg–rich region or RGG motif, where the Arg residues are preferentially methylated in several proteins (Fig. 2*C*) (36). Like K18, K8 also contained a potential methylation site in RGG motif (GSSNF^{47}RGGLGGG) located in the head domain, which was not detected in our mass spectrometry analysis or other prior proteomic studies. Methylation mutants for K8 Arg47 and K18 Arg55 (Arg-to-Ala or Arg-to-Lys) were generated and cotransfected with the combination of their counterpart keratin WT. Methylated proteins were immunoprecipitated with anti-MeR specific Ab, followed by immunoblotting with K8 or K18 Ab (Fig. 2*D*). No significant decrease in the detected amount of keratins between WT and the mutants was observed (Fig. 2*D*). This was likely due to the binding of anti-MeR Ab with methylated Arg residue in cotransfected counterpart keratin WT that formed obligate heteropolymers with methylation mutant. However, the amount of K8 and K18 detected by anti-MeR Ab was dramatically reduced when the mutant K8 was cotransfected with mutant K18 [*i.e.*, K8 R47A/ K18 R55A or K8 R47K/ K18 R55K (Fig. 2*E*)]. The mutational analysis supports the mass spectrometry data and indicates that K8 Arg47 and K18 Arg55 are major MMA sites. Because the monomethylation was regarded as an intermediate in the formation of dimethyl-Arg, we examined whether K8 and K18 contained dimethyl-Arg. Keratin immunoprecipitates were prepared and immunoblotted with symmetric or asymmetric di-MeR antibodies. However, we could not detect asymmetrically dimethylated Arg or symmetrically dimethylated Arg in the immunoprecipitated keratins (Supplemental Fig. S4). Given the K8 Arg47 and K18 Arg55 sites are localized in the head domain of keratins (where phosphorylation occurred on Ser74 in K8 and Ser53 in K18), the potential effect of methylation on keratin phosphorylation was investigated. As shown in Fig. 2*D*, the phosphorylation levels of the sites (K8 Ser74 and K18 Ser53) on methylation mutant keratins were similar to the level of WT keratins.

In addition, we examined whether the mutations of acetylated sites and methylated sites in K8 and K18 had an effect on keratin filament organization. The immunostained filament patterns of keratin WT and the mutants were indistinguishable (Supplemental Fig. S5). The mutant keratins formed what appeared to be normal filament organization under basal conditions.

Effect of acetylation and methylation on keratin stability

Studies have shown that Lys acetylation and Arg methylation are associated with protein stability (11, 14, 31, 37). Here, we examined the effect of acetylation/methylation on the stability of keratin proteins. The BHK cells were cotransfected with a set of K8 and K18 WT, acetylation mutants, or methylation mutants, and then treated with CHX to inhibit *de novo* protein synthesis (**Fig. 3**). After 60 h, K8 WT and K18 WT were degraded by about 18 and 37%, respectively, whereas acetylation mutant K8, K108R or K207R, and the double mutant K18, K187/426R, were degraded by about 40 and 5%, respectively (Fig. 3*A, B*). However, after the CHX treatment for 60 h, the amount of methylation mutant proteins was dramatically reduced with 50–80% degradation of the mutant K8, R47A/K, and 70–80% degradation of the mutant K18, R55A/K (Fig. 3*A, C*). Taken together, these results suggest that Arg methylation on keratins is a major factor regulating the stability of keratin proteins and that Lys acetylation has only a limited effect on keratin protein stability.

Because Arg methylation on keratins modulates the keratin protein stability, we examine the effect of methylation inhibitors on the keratin filament formation. We first tested several methyltransferase inhibitors to determine which methyltransferases were involved in keratin methylation. Among them, AdOx, known as a global methyltransferase inhibitor (29, 31), significantly reduced the keratin methylation (Fig. 3*D*). However, specific PRMT inhibitors (29, 30, 32, 38), such as AMI-1, MS049, and GSK591, showed the limited effect on the inhibition of keratin

with other proteins known to be methylated. RGG and RG sequences are highlighted in gray. hnRNP A1, heterogeneous nuclear RNP A1; hnRNP K, heterogeneous nuclear RNP K; TAF15, TATA-box binding protein associated factor 15; ERa, estrogen receptor α; p53, tumor protein 53; Smad6, smad family member 6; asterisk, Arg residue modified by methylation; aDMA, asymmetric dimethylated Arg; sDMA, symmetric dimethylated Arg. *D*) BHK cells were cotransfected with either combination of K18 WT and K8 methylation mutant construct (K8 R47A or R47K) or the combination of K8 WT and K18 methylation mutant construct (K18 R55A or R55K). Levels of MMA K8 and K18 were verified by immunoprecipitation using anti-MeR Ab, followed by immunoblot with anti-K8/K18 Ab. MMA proteins were used as loading control. *E*) BHK cells were transfected with K8 and 18 WT, or combination of methylation mutant K8 and K18 mutant construct. Transfected cells were analyzed as described in *D*. The graph represents means ± SD of 3 independent experiments. $*P < 0.05$, $**P < 0.005$, $***P < 0.0005$.

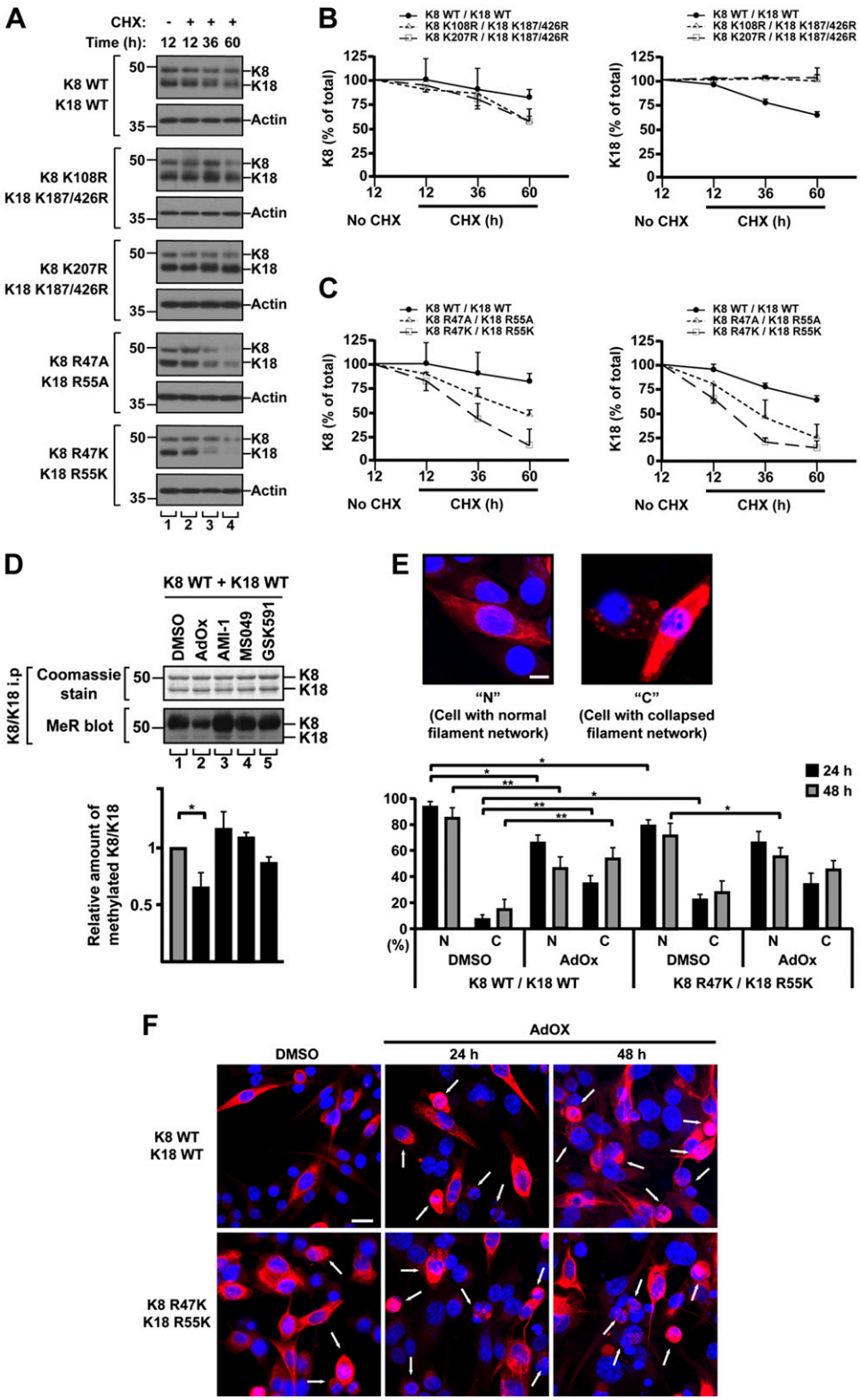

Figure 3. Mutation of acetylation or methylation sites on keratins alters their protein stability. *A*) BHK cells were cotransfected with indicated keratin constructs and treated with CHX for 12, 36, or 60 h. Total lysates were separated by SDS-PAGE, followed by immunoblotting with anti-K8/K18 Ab. *B*, *C*) Quantity of K8 and K18 normalized by actin quantitatively analyzed by densitometry. Graph represented as means ± SD. Note: stability of acetylation mutant K8 and K18 showed a limited change, compared with WT, but methylation mutants K8 and K18 exhibited significant reduction in both Arg-to-Ala and Arg-to-Lys mutants, compared with WT. *D*) BHK cells were transfected with K8 and K18 WT and then were treated with DMSO as a solvent control or the indicated methylation inhibitors for 48 h. Levels of methylated K8 and K18 were verified by immunoprecipitation using anti-K8/K18 Ab, followed by immunoblotting with anti-MeR Ab. Note that the level of keratin methylation was dramatically decreased after AdOX treatment. The graph represents means ± SD from 3 independent experiments. $^*P < 0.05$. *E*) BHK cells were cotransfected with the indicated keratin constructs and were treated with DMSO or AdOX (20 μM) for 24 or 48 h. The cells were then fixed and stained with anti-K8/K18 Ab (red) and DAPI (blue). Images were obtained using fluorescence microscopy equipped with a 40 × /1.3 oil objective lens. Cells with normal (N) filament network and cells with collapsed (C) filament network were counted in 2–3 independent experiments, and at least 55 cells were counted per each experiment. Graph shows the % ratio of N and C cells and represents the means ± SD. Scale bar, 10 μm. $^*P < 0.05$, $^{**}P < 0.005$. *F*) Representative confocal images of Fig. 2*E*. Arrows indicate C cells. Scale bar, 20 μm.

methylation under tested conditions (Fig. 3*D* and Supplemental Fig. S6). It is likely, at least in part, that the keratins are methylated by methyltransferases other than PRMTs, such as NADH:ubiquinone oxidoreductase complex assembly factor 7 (NDUFAF7, a protein arginine methyltransferase). We then performed the time course experiment of immunostaining to compare the filament organization between WT and methylation-deficient keratin mutant with or without AdOx. The ratio of cells with a normal (N) filament network or a collapsed (C) filament

network was compared (Fig. 3*E*, *F*). The AdOx treatment caused markedly increased C cells in BHK cells transfected with K8/K18 WT (about 35~50% of C cells), which indicated that keratin methylation was important for the filament organization. However, the effect of AdOx was not dramatic in BHK cells transfected with methylation-deficient keratin mutant as compared with the cells with K8/K18 WT. Indeed, under the DMSO-treated control condition, the BHK cells with K8/K18 WT contained about 10% of C cells, whereas the BHK cells with the keratin mutant showed about 25% of C cells (Fig. 3*E*). It is likely due to instability of the mutant protein as shown in Fig. 3*A*, *C*. Notably, as shown in Supplemental Fig. S5, the methylation-deficient keratin mutant initially forms a normal filament network as compared with K18 R90C, a positive control to show the filament disruption (dot/inclusion-like patterns) in all transfected cells.

Because of the known involvement of the ubiquitin-proteasome pathway in keratin degradation (39), and given that we found an association between keratin methylation and keratin protein stability (Fig. 3*A*, *C*), we compared the level of ubiquitination in keratin WT to that of methylation mutants in the presence of proteasome inhibitors *N*-acetyl-Leu-Leu-norleucinal (ALLN) or carbobenzoxy-Leu-Leu-leucinal (MG132, an inhibitor of the 26S proteasome complex) (Supplemental Fig. S7). The ubiquitination level of methylation mutant was similar to the level of WT, which indicates that the protein instability of mutant keratin is not caused by their enhanced ubiquitination.

Effects of liver disease–associated keratin mutations on their acetylation/methylation

Studies showed that some liver disease–associated keratin mutations resulted in the alteration of keratin phosphorylation such as the inhibited phosphorylation at K8 Ser74 or Ser432 residue in the liver disease–associated mutation K8 G62C or G434S, respectively (4, 10). Here, we tested whether the keratin mutations associated with liver diseases affect keratin acetylation or methylation. Human liver disease–related K8 and K18 variants (Y54H, G62C, R341H, G434S, I466fs in K8 and Δ65-72, I150V in K18) were selected based on their prevalence in human liver disease, their biochemically different properties (40), and their position near the acetylation or methylation sites (**Fig. 4**). Keratin variants were cotransfected with a counterpart keratin that was mutated at acetylation or methylation site(s) to minimize the binding of a counterpart keratin with anti-AcK or anti-MeR Ab that generated obligate heteropolymers with each keratin variant. Acetylation of tested keratin variants increased by 1.2–2.2-fold, with the exception of the K8 G434S variant, which showed a dramatic inhibition of acetylation (**Fig. 5*A*, *B***). We observed the inhibition of acetylation in K8 G434S when the K8 mutant was cotransfected with K18 acetylation mutant (Fig. 5*A*) but not with K18 WT (Supplemental Fig. S8). It is likely that the cotransfected K18 WT forms heteropolymers with K8 G434S and the acetylated residue of K18 WT is recognized by anti-AcK Ab. Therefore, the effect of K8 G434S mutation on K8 acetylation could not be observed in this immunoprecipitation experiment by using anti-AcK Ab. A potential limitation of this finding is that the experiment was carried out in cotransfected BHK cell systems with K8-G434S and K18-K187R/K426R, and the Lys at position 187 and 426 on K18 undergo several different modifications (acetylation, ubiquitination, sumoylation, methylation, and succinylation) based on data from *www.phosphosite.org*, which may also contribute to the lack of acetylation of the K8 G434S (Fig. 5*A*). The PTM status of liver disease keratin variants in the context of its WT partner keratin by using nano-LC/MS and generating site-specific PTM antibodies remains to be confirmed.

In terms of the modulation of liver disease–associated keratin variants, K8 variants showed a minor change of

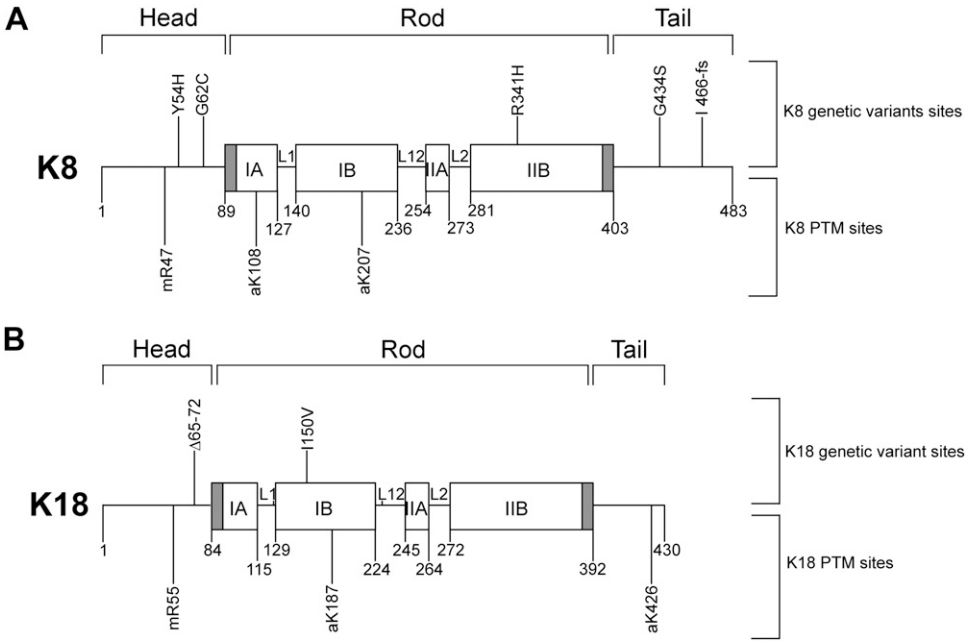

Figure 4. Schematic diagram representing human liver disease-related keratin variants and acetylation/methylation sites in K8 and K18. Keratin proteins are composed of 3 domains: conserved α-helical rod domain flanked by nonhelical head and tail domains. Rod domain is composed of subdomains IA, IB, IIA, and IIB, connected by linker1 (L1), linker12 (L12), and linker2 (L2). Shaded region within IA and IIB indicates highly conserved region. Previously described genetic variants of K8 (*A*) and K18 (*B*) related to liver diseases (50, 51). PTM sites examined herein. a, acetylation; m, methylation.

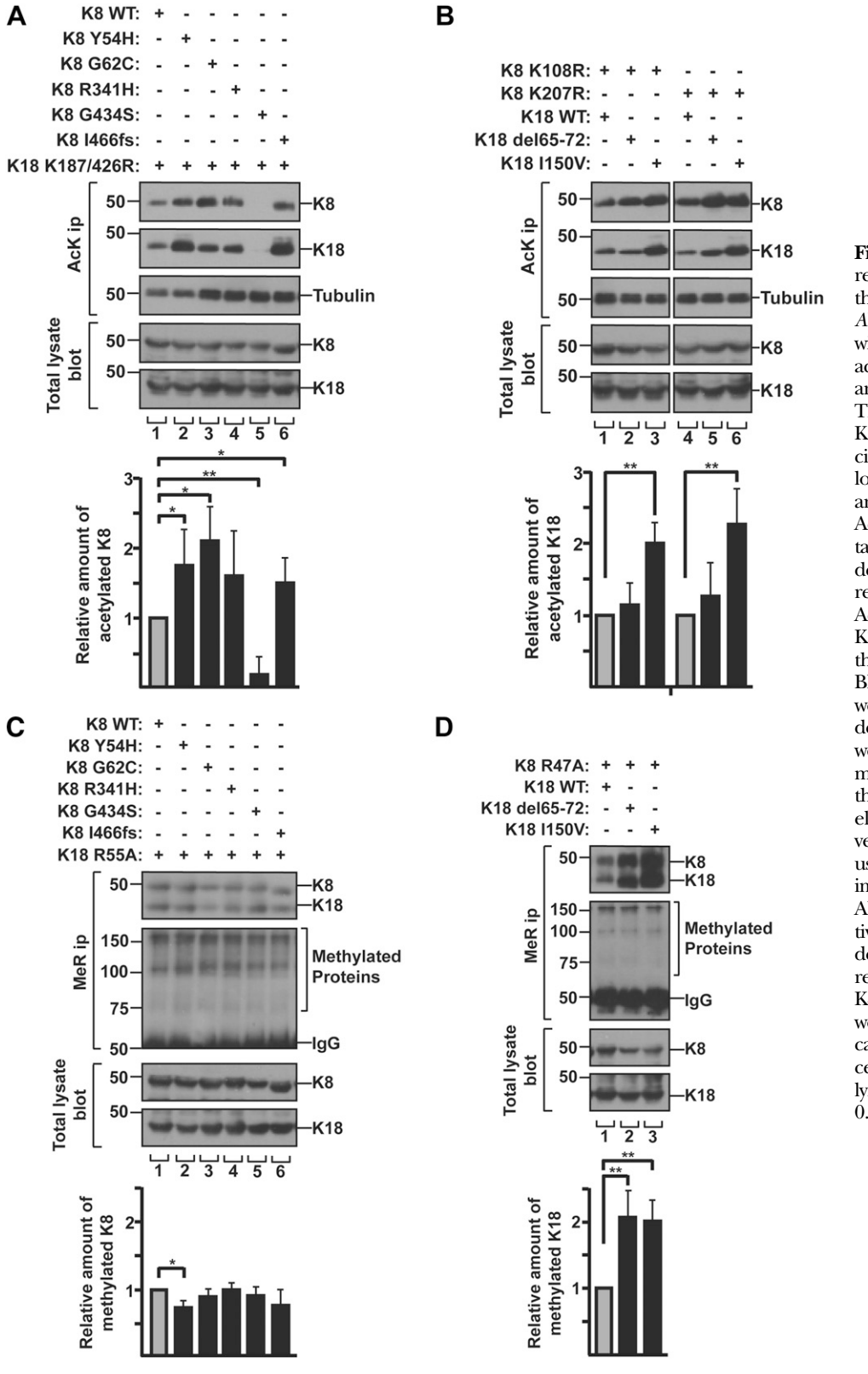

Figure 5. Human liver disease–related keratin mutations alter the acetylation/methylation state. *A*) BHK cells were cotransfected with the combination of K18 acetylation mutant K187/426R and indicated K8 constructs. The level of acetylated K8 and K18 was verified by immunoprecipitation using anti-AcK Ab, followed by immunoblotting with anti-K8 and anti-K18 antibodies. Acetylated keratins were quantitatively analyzed after 3 independent experiments. Results are represented as means ± SD. *B*) Acetylation mutant K8 K108R or K207R were cotransfected with the indicated K18 constructs in BHK cells. Acetylated keratins were quantitatively analyzed as described in *A*. *C*) BHK cells were cotransfected with K18 methylation mutant R55A and the indicated K8 constructs. Levels of MMA K8 and K18 were verified by immunoprecipitation using anti-MeR Ab, followed by immunoblot with anti-K8/K18 Ab. MMA keratins were quantitatively analyzed after 3 independent experiments. Results are represented as means ± SD. *D*) K8 methylation mutant R47A were transfected with the indicated K18 constructs in BHK cells. Transfected cells were analyzed as described in *C*. $^*P < 0.05$, $^{**}P < 0.005$.

methylation levels, compared with K8 WT (Fig. 5C), whereas methylation of K18 variants, Δ65-72 and I150V, was enhanced by nearly 2-fold (Fig. 5*D*). Given that Arg methylation on keratins is involved in the up-regulation of keratin protein stability (Fig. 3), we investigated the effect of K18 Δ65-72 or I150V mutation on the protein stability. After 60 h of CHX treatment, the quantity of protein was reduced by 40–50% in case of K18 WT or Δ65-72, but <10% in K18 I150V (**Fig. 6*A*, *B***). These results indicate that the K18 I150V mutation had a more dramatic effect on the enhanced protein stability than did Δ65-72. This is likely, at least in part, due to the different levels of PTMs in each

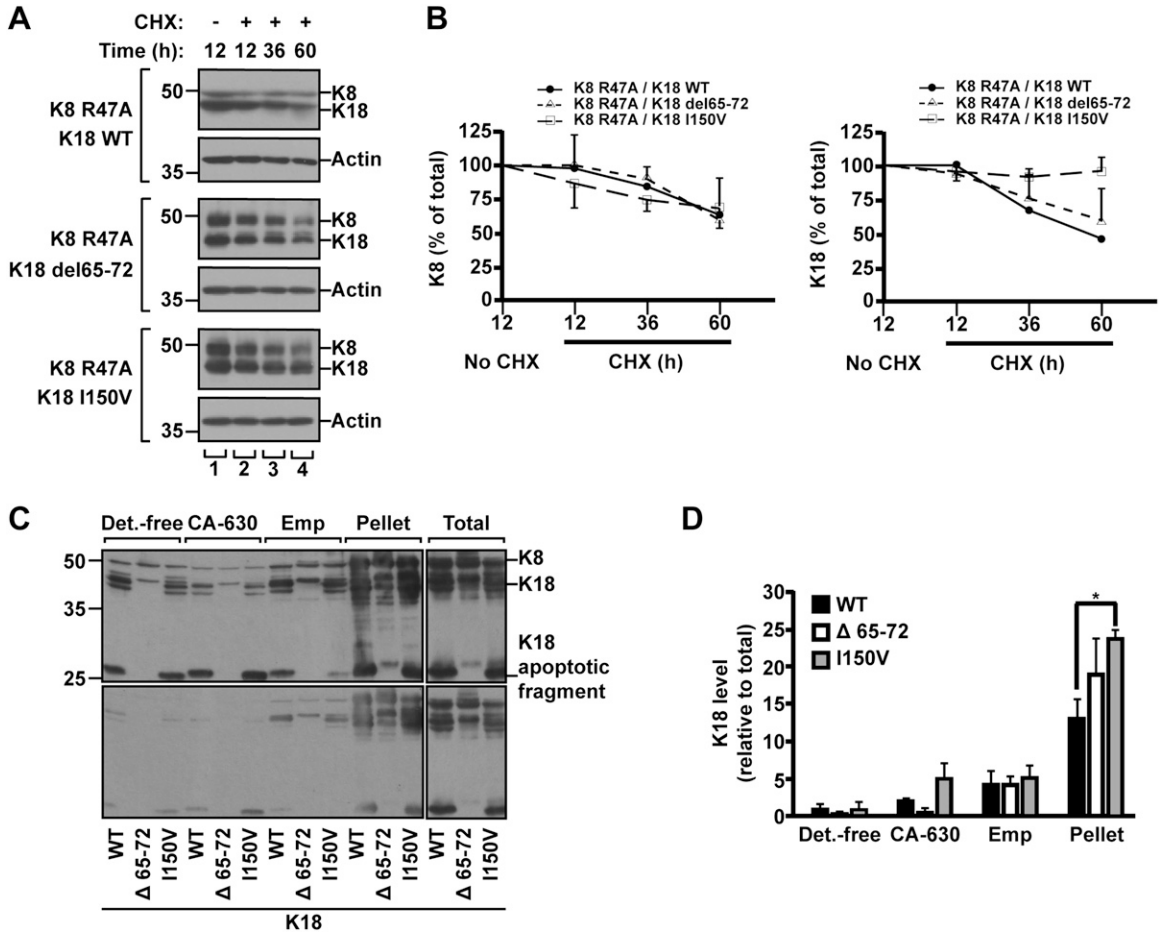

Figure 6. Protein stability and solubility of highly methylated human liver disease–related K18 variants. *A*, *B*) BHK cells transfected with the indicated keratin constructs were incubated with CHX for 12, 36, or 60 h. Total lysates were separated by SDS-PAGE, followed by immunoblotting with anti-K8/K18 Ab (*A*). Amounts of K8 and K18 were quantitatively analyzed by densitometry, and graphs were represented as means ± SD (*B*). *C*, *D*) BHK cells were cotransfected with a combination of indicated K18 constructs together with K8 WT. Transfected cells were used for the preparation of sequential subcellular fractions (15). Detergent-free buffer (Det.-free), nonionic (CA-630), ionic (Emp) detergent, remaining pellet and total lysates sample were prepared. Total lysates and cell fractions were separated by SDS-PAGE, followed by immunoblotting with anti-K8/K18 Ab. *C*) Upper and lower panels represent long and short exposures of the immunoblotted membrane, respectively. *D*) Amounts of K8/K18 and K18 human variants were quantitatively analyzed by densitometry. Note: K18 I150V variant showed significant increase in insoluble pellet fraction compared with K18 WT. The graph represents the means ± SD of 3 independent experiments. $^*P < 0.05$.

variant. The K18 I150V mutation increased both acetylation and methylation, whereas K18 Δ65-72 mutation up-regulated mainly methylation (Fig. 5*B*, *D*). We speculate that the additional acetylation on highly methylated keratins provides a synergistic effect to prolong protein stability. The overall results of keratin acetylation/methylation and protein stability are summarized in **Table 2**.

To assess the relationship between prolonged keratin stability and solubility, we analyzed K18 in cytosolic, Igepal CA630-solubilized, Empigen BB-solubilized, and remaining non-Empigen BB-solubilized cell fractions that were sequentially separated from K18 variant-transfected cells. As shown in Fig. 6*C*, *D*, the K18 I150V variant showed prolonged protein stability, exhibiting a significant increase in the insoluble pellet fraction compared with K18 WT. Taken together, our results suggest that liver disease–associated keratin mutations resulting in alteration of PTM levels may contribute to prolonged keratin turnover in a mutation-selective fashion.

DISCUSSION

PTMs are important for the functions of keratins (7, 9). Specifically, phosphorylation and glycosylation of K8 and K18 are well-studied *in vitro* cultured cell systems as well as *in vivo* mouse models (7–9). However, other PTMs of keratins, including Lys acetylation and Arg methylation, have been mainly studied by proteomic analysis (11, 12, 14, 18, 19), and thus the functional significances of the identified PTM sites have not been fully studied. Here, we identified K8 Lys108 and K18 Lys187/426 for acetylation sites, and K8 Arg47 and K18 Arg55 for methylation sites by site-directed mutagenesis assay combined with nano-LC-MS/MS (Fig. 2 and Table 1). Interestingly, inhibition of Arg methylation on K8 and K18 caused rapid degradation of keratin proteins (Fig. 3*A*, *C*), which suggests that Arg methylation enhances the protein stability of keratins. Further, we observed a range of increased acetylation on liver disease–associated K8 and K18 variants with

TABLE 2. *Keratin acetylation/methylation and protein stability*

Variant	Mutations in acetylation sites	Mutations in methylation sites	Liver disease-associated keratin mutants	
			K8 mutants	K18 mutants
K8/K18 constructs	K8 K108R, K8 K207R, K18 K187/426R	K8 R47K/A, K18 R55K/A	Y54H, G62C, R341H, G434S, I466fs	del65-72, I150V
Acetylation	↓	ND	K8 G434S[b] ↓ Other mutants[b] ↑	K18 del65-72 ↔ K18 I150V[b] ↑
Methylation	ND	↓	K8 mutants ↔	K18 del65-72[b] ↑ K18 I150V[b] ↑
Keratin stability	K8 K108R ↔ K8 K207R ↔ K18 K187/426R ↔	K8 R47K/A[b] ↓ K18 R55K/A[b] ↓	ND[a]	K18 del65-72[b] ↑ K18 I150V[b] ↑

Note that K18 I150V mutation increased both acetylation and methylation, whereas K18 del65–72 mutation up-regulated mainly methylation. It is speculated that additional acetylation on highly methylated keratins has a synergistic effect on prolonged protein stability. ND, not determined. [a]Because liver disease–associated K8 mutants showed the similar level of methylation as compared with that of K8 WT (Fig. 5*C*), the keratin stability was not examined. [b]The significant change of indicated level. Symbols indicated ↓ decrease, ↑ increase, and ↔ no significant change as compared with WT.

1 exception: the K8 G434S variant, which showed significantly decreased acetylation (Fig. 5*A, B*). Notably, the highly acetylated/methylated K18 I150V variant had unusually prolonged protein stability (Figs. 5 and 6 and Table 2). One potential limitation of our study is that the work was carried out in transfected cell systems and the PTMs we identified were not assessed in nonmanipulated systems.

Since the finding of Lys acetylation sites on keratins from the large scale of proteomics studies (11, 12), 1 study reported the physiologic role of acetylated K8 at Lys207 residue, which decreased keratin solubility and regulated the formation of filament networks (15). Here, we identified an acetylation site on K8, Lys108, as one of the major acetylation sites (Fig. 2), and blocking acetylation at the site (Lys108 to Arg mutation) caused about a 20% reduction of K8 Ser74 phosphorylation (Supplemental Fig. S3). This indicates that K8 Lys108 acetylation may have effects on keratin filament organization and solubility. This supports other published report about K8 Lys207 acetylation (15). However, the K8 Lys108/207 and K18 Lys187/426 acetylation had a limited effect on the stability of keratin proteins (Fig. 3*A, B*).

Deregulation of acetylation is involved in various human diseases, including Parkinson's disease, metabolic disorders such as obesity and diabetes, and liver diseases (41, 42). Lys deacetylase inhibitors ameliorate disease progression in several models of the diseases. For example, Sirtuin 2 (SIRT2) inhibitors were shown to protect dopaminergic neurons from α-synuclein-mediated toxicity and modify aggregation in models of Parkinson's disease (43). A study further demonstrated the deregulation of keratin acetylation in hyperglycemic conditions (15). Increased K8 acetylation was detected in diabetic *ob/ob* mouse liver and diabetic human liver tissue. This suggests that the increased acetylation may occur during liver damage related to diabetes (15). In the present study, we observed the enhanced acetylation on the tested keratin variants associated with liver diseases, with the exception of the K8 G434S variant, which was significantly diminished in its acetylation (Fig. 5*A*). Although we do not yet understand the mechanisms of how deregulated keratin acetylation modulates the biochemical properties of keratin, K8 G62C and K8 R341H variants both showed enhanced acetylation (Fig. 5*A*) and both variants predisposed transgenic mice to liver injury (10, 44).

Arg methylation on keratins is poorly understood compared with other PTMs. Previous proteomic analysis demonstrated Arg methylation of K1, K2a, and K9, without precise information on sites (17). Another proteomic study revealed multiple potential Arg-methylated sites on K1, K8, K18, K19, and K20, among over 1000 Arg-methylated sites that were identified on numerous proteins in human cell line, alhough the potential Arg-methylated sites remain to be verified biochemically (19). We performed biochemical and functional experiments for Arg methylation on keratins that have not been fully studied, some of which have not been previously examined at all. We clearly demonstrated that K8 Arg47 and K18 Arg55 are major methylation sites (Fig. 2*E*). Furthermore, we demonstrated that blocking the methylation (Arg-to-Lys/Ala mutation) led to a rapid degradation of keratins, which indicates that Arg methylation of keratins increased protein stability (Fig. 3*A, C*). Interestingly, in studies with Kruppel-like factor 4 (KLF4, a zinc-finger transcription factor), it has been found that Arg methylation interfered with KLF4 ubiquitination and enhanced protein stability (45). In addition, methylated Axis inhibition protein 1 (Axin 1, a negative regulator of Wnt signaling) by PRMT1 enhanced its stability (31), and methylation mutant of Signal transducer and activator of transcription 6 (STAT6, a transcription factor of cytokine signaling) is more instable than STAT6 WT (46). Thus, it is likely that the high level of methylation of keratins may provide increased protein stability and may protect from protein degradation. However, in our study, we did not detect increased ubiquitination of keratin methylation mutants, K8 R47A and K18 R55A (Supplemental Fig. S7). It is likely that the rapid turnover of the keratin mutants is independent of ubiquitin-proteasome pathway. On the other hand, liver disease–associated K18 variants Δ65-72

and I150V showed a significant increase in levels of methylation and a prolonged half-life of their respective proteins. These results indicate that the liver disease–associated keratin mutations could be involved in the regulation of keratin protein stability, leading to unbalanced K8 to K18 ratios, resulting in the formation of keratin aggregates.

Mallory-Denk bodies are hepatocyte inclusions found in a range patients with chronic liver diseases, and K8 and K18 are major IF proteins found in the inclusions (22). The mechanism of MDB formation is becoming understood. The formation of MDBs occurs when the ratio of K8 to K18 is increased (*i.e.*, K8 > K18 protein state), which is regulated by keratin induction and modifications, such as ubiquitination, phosphorylation, and transamidation (3). Studies have demonstrated that K8 or K18 overexpression in transgenic mice predisposed or blocked MDB formation, respectively (22, 47). This suggests that the balance between levels of K8 and K18 plays an important role in the formation of MDBs. Keratins found in MDBs are ubiquitinated and hyperphosphorylated (48, 49), and the stress-mediated phosphorylation of K8 S74 induces K8 cross-linking by transglutaminase-2, leading to MDB formation (25). In addition, transgenic mice that express K8 S74A, phosphomutant, or K8 G62C liver disease variant, which inhibits phosphorylation of K8 S74, showed the reduced ability of MDB formation (25). Studies focusing on the relationship between keratin phosphorylation/transamidation and the formation of MDBs in liver cells show that the MDB formation is closely linked with dysregulated expression, hyperphosphorylation, and cross-linking of keratins (21). However, the roles of keratin acetylation and methylation related to MDB formation and liver diseases have not yet been determined.

A study about keratin acetylation reported that acetylation at K8 Lys207 was up-regulated by hyperglycemia and down-regulated by SIRT2 (15). Furthermore, the keratin acetylation regulated filament organization by modulating phosphorylation at K8 S74 residue (15). In our study, we identified 3 additional acetylation sites in keratins: Lys108 on K8, and Lys187 and 426 on K18. As noted in a previous study, there is a likely correlation between the acetylation and phosphorylation of keratins (15). For example, mutation at K8 acetylation sites K108R or K207R interfered with phosphorylation at K8 S74 residue (Supplemental Fig. S3), and K8 acetylation was blocked in the K8 G434S variant, which is a liver disease–associated K8 variant known to disrupt phosphorylation at K8 S432 residue (Fig. 5*A*). A key achievement of this study is that we demonstrated the importance of keratin methylation in the turnover of keratins. Mutations at keratin methylation sites K8 R47A/K and K18 R55A/K caused the decreased stability of keratin protein (Fig. 3), whereas the highly methylated liver disease–associated K18 mutations, notably K18 I150V, showed less solubility and prolonged stability of the variant protein that may lead to an unbalanced K8 and K18 ratio (Fig. 6). Together with keratin phosphorylation/transamidation, keratin acetylation/methylation may be involved in modulating the formation of MDBs by altering phosphorylation and turnover of K8 and K18 in liver. FJ

ACKNOWLEDGMENTS

This work was supported by the Korean Ministry of Education, Science, and Technology Grants 2016R1A2B4012808 and 2018R1D1A1A02086060, the Yonsei University Research Fund 2018-22-0072 (to N.-O.K.), and the National Research Foundation of Korea funded by the Ministry of Science and Information and Communication Technology (ICT) Grant NRF-2016R1A5A1010764 (to J.-W.C.). The authors declare no conflicts of interest.

AUTHOR CONTRIBUTIONS

K.-H. Jang, H.-N. Yoon, J. Lee, H. Yi, S.-Y. Park, S.-Y. Lee, Y. Lim, and H.-J. Lee performed experiments and analyzed data; K.-H. Jang, H.-N. Yoon, and N.-O. Ku designed the experiments; K.-H. Jang, H.-N. Yoon, H. Yi, and N.-O. Ku wrote the manuscript; and J.-W. Cho, Y.-K. Paik, and W. S. Hancock contributed analytic tools.

REFERENCES

1. Eriksson, J. E., Dechat, T., Grin, B., Helfand, B., Mendez, M., Pallari, H. M., and Goldman, R. D. (2009) Introducing intermediate filaments: from discovery to disease. *J. Clin. Invest.* **119**, 1763–1771
2. Schweizer, J., Bowden, P. E., Coulombe, P. A., Langbein, L., Lane, E. B., Magin, T. M., Maltais, L., Omary, M. B., Parry, D. A., Rogers, M. A., and Wright, M. W. (2006) New consensus nomenclature for mammalian keratins. *J. Cell Biol.* **174**, 169–174
3. Ku, N. O., Strnad, P., Zhong, B. H., Tao, G. Z., and Omary, M. B. (2007) Keratins let liver live: mutations predispose to liver disease and crosslinking generates Mallory-Denk bodies. *Hepatology* **46**, 1639–1649
4. Omary, M. B., Ku, N. O., Strnad, P., and Hanada, S. (2009) Toward unraveling the complexity of simple epithelial keratins in human disease. *J. Clin. Invest.* **119**, 1794–1805
5. Ku, N. O., Strnad, P., Bantel, H., and Omary, M. B. (2016) Keratins: biomarkers and modulators of apoptotic and necrotic cell death in the liver. *Hepatology* **64**, 966–976
6. Herrmann, H., Strelkov, S. V., Burkhard, P., and Aebi, U. (2009) Intermediate filaments: primary determinants of cell architecture and plasticity. *J. Clin. Invest.* **119**, 1772–1783
7. Omary, M. B., Ku, N. O., Tao, G. Z., Toivola, D. M., and Liao, J. (2006) "Heads and tails" of intermediate filament phosphorylation: multiple sites and functional insights. *Trends Biochem. Sci.* **31**, 383–394
8. Ku, N. O., Toivola, D. M., Strnad, P., and Omary, M. B. (2010) Cytoskeletal keratin glycosylation protects epithelial tissue from injury. *Nat. Cell Biol.* **12**, 876–885
9. Snider, N. T., and Omary, M. B. (2014) Post-translational modifications of intermediate filament proteins: mechanisms and functions. *Nat. Rev. Mol. Cell Biol.* **15**, 163–177
10. Ku, N. O., and Omary, M. B. (2006) A disease- and phosphorylation-related nonmechanical function for keratin 8. *J. Cell Biol.* **174**, 115–125
11. Zhao, S., Xu, W., Jiang, W., Yu, W., Lin, Y., Zhang, T., Yao, J., Zhou, L., Zeng, Y., Li, H., Li, Y., Shi, J., An, W., Hancock, S. M., He, F., Qin, L., Chin, J., Yang, P., Chen, X., Lei, Q., Xiong, Y., and Guan, K. L. (2010) Regulation of cellular metabolism by protein lysine acetylation. *Science* **327**, 1000–1004
12. Choudhary, C., Kumar, C., Gnad, F., Nielsen, M. L., Rehman, M., Walther, T. C., Olsen, J. V., and Mann, M. (2009) Lysine acetylation targets protein complexes and co-regulates major cellular functions. *Science* **325**, 834–840
13. Westermann, S., and Weber, K. (2003) Post-translational modifications regulate microtubule function. *Nat. Rev. Mol. Cell Biol.* **4**, 938–947
14. Kim, S. C., Sprung, R., Chen, Y., Xu, Y., Ball, H., Pei, J., Cheng, T., Kho, Y., Xiao, H., Xiao, L., Grishin, N. V., White, M., Yang, X. J., and Zhao, Y. (2006) Substrate and functional diversity of lysine acetylation revealed by a proteomics survey. *Mol. Cell* **23**, 607–618
15. Snider, N. T., Leonard, J. M., Kwan, R., Griggs, N. W., Rui, L., and Omary, M. B. (2013) Glucose and SIRT2 reciprocally mediate the regulation of keratin 8 by lysine acetylation. *J. Cell Biol.* **200**, 241–247

16. Bedford, M. T., and Clarke, S. G. (2009) Protein arginine methylation in mammals: who, what, and why. *Mol. Cell* **33**, 1–13
17. Boisvert, F. M., Côté, J., Boulanger, M. C., and Richard, S. (2003) A proteomic analysis of arginine-methylated protein complexes. *Mol. Cell. Proteomics* **2**, 1319–1330
18. Bremang, M., Cuomo, A., Agresta, A. M., Stugiewicz, M., Spadotto, V., and Bonaldi, T. (2013) Mass spectrometry-based identification and characterisation of lysine and arginine methylation in the human proteome. *Mol. Biosyst.* **9**, 2231–2247
19. Guo, A., Gu, H., Zhou, J., Mulhern, D., Wang, Y., Lee, K. A., Yang, V., Aguiar, M., Kornhauser, J., Jia, X., Ren, J., Beausoleil, S. A., Silva, J. C., Vemulapalli, V., Bedford, M. T., and Comb, M. J. (2014) Immunoaffinity enrichment and mass spectrometry analysis of protein methylation. *Mol. Cell. Proteomics* **13**, 372–387
20. Omary, M. B. (2017) Intermediate filament proteins of digestive organs: physiology and pathophysiology. *Am. J. Physiol. Gastrointest. Liver Physiol.* **312**, G628–G634
21. Strnad, P., Paschke, S., Jang, K. H., and Ku, N. O. (2012) Keratins: markers and modulators of liver disease. *Curr. Opin. Gastroenterol.* **28**, 209–216
22. Zatloukal, K., French, S. W., Stumptner, C., Strnad, P., Harada, M., Toivola, D. M., Cadrin, M., and Omary, M. B. (2007) From Mallory to Mallory-Denk bodies: what, how and why? *Exp. Cell Res.* **313**, 2033–2049
23. Afifiyan, N., Tillman, B., French, B. A., Masouminia, M., Samadzadeh, S., and French, S. W. (2017) Over expression of proteins that alter the intracellular signaling pathways in the cytoplasm of the liver cells forming Mallory-Denk bodies. *Exp. Mol. Pathol.* **102**, 106–114
24. Liao, J., Ku, N. O., and Omary, M. B. (1997) Stress, apoptosis, and mitosis induce phosphorylation of human keratin 8 at Ser-73 in tissues and cultured cells. *J. Biol. Chem.* **272**, 17565–17573
25. Kwan, R., Hanada, S., Harada, M., Strnad, P., Li, D. H., and Omary, M. B. (2012) Keratin 8 phosphorylation regulates its transamidation and hepatocyte Mallory-Denk body formation. *FASEB J.* **26**, 2318–2326
26. Ku, N. O., Toivola, D. M., Zhou, Q., Tao, G. Z., Zhong, B., and Omary, M. B. (2004) Studying simple epithelial keratins in cells and tissues. *Methods Cell Biol.* **78**, 489–517
27. Schölz, C., Weinert, B. T., Wagner, S. A., Beli, P., Miyake, Y., Qi, J., Jensen, L. J., Streicher, W., McCarthy, A. R., Westwood, N. J., Lain, S., Cox, J., Matthias, P., Mann, M., Bradner, J. E., and Choudhary, C. (2015) Acetylation site specificities of lysine deacetylase inhibitors in human cells. *Nat. Biotechnol.* **33**, 415–423
28. Yamamoto, T., Takano, N., Ishiwata, K., and Suematsu, M. (2011) Carbon monoxide stimulates global protein methylation via its inhibitory action on cystathionine β-synthase. *J. Clin. Biochem. Nutr.* **48**, 96–100
29. Hou, W., Nemitz, S., Schopper, S., Nielsen, M. L., Kessels, M. M., and Qualmann, B. (2018) Arginine methylation by PRMT2 controls the functions of the actin nucleator Cobl. *Dev. Cell* **45**, 262–275.e8
30. Clarke, T. L., Sanchez-Bailon, M. P., Chiang, K., Reynolds, J. J., Herrero-Ruiz, J., Bandeiras, T. M., Matias, P. M., Maslen, S. L., Skehel, J. M., Stewart, G. S., and Davies, C. C. (2017) PRMT5-dependent methylation of the TIP60 coactivator RUVBL1 is a key regulator of homologous recombination. *Mol. Cell* **65**, 900–916.e7
31. Cha, B., Kim, W., Kim, Y. K., Hwang, B. N., Park, S. Y., Yoon, J. W., Park, W. S., Cho, J. W., Bedford, M. T., and Jho, E. H. (2011) Methylation by protein arginine methyltransferase 1 increases stability of Axin, a negative regulator of Wnt signaling. *Oncogene* **30**, 2379–2389
32. Bonham, K., Hemmers, S., Lim, Y. H., Hill, D. M., Finn, M. G., and Mowen, K. A. (2010) Effects of a novel arginine methyltransferase inhibitor on T-helper cell cytokine production. *FEBS J.* **277**, 2096–2108
33. Shen, Y., Szewczyk, M. M., Eram, M. S., Smil, D., Kaniskan, H. U., de Freitas, R. F., Senisterra, G., Li, F., Schapira, M., Brown, P. J., Arrowsmith, C. H., Barsyte-Lovejoy, D., Liu, J., Vedadi, M., and Jin, J. (2016) Discovery of a potent, selective, and cell-active dual inhibitor of protein arginine methyltransferase 4 and protein arginine methyltransferase 6. *J. Med. Chem.* **59**, 9124–9139
34. Liao, J., and Omary, M. B. (1996) 14-3-3 proteins associate with phosphorylated simple epithelial keratins during cell cycle progression and act as a solubility cofactor. *J. Cell Biol.* **133**, 345–357
35. Hatzfeld, M., and Weber, K. (1990) The coiled coil of *in vitro* assembled keratin filaments is a heterodimer of type I and II keratins: use of site-specific mutagenesis and recombinant protein expression. *J. Cell Biol.* **110**, 1199–1210
36. Kim, S., Merrill, B. M., Rajpurohit, R., Kumar, A., Stone, K. L., Papov, V. V., Schneiders, J. M., Szer, W., Wilson, S. H., Paik, W. K., and Williams, K. R. (1997) Identification of N(G)-methylarginine residues in human heterogeneous RNP protein A1: Phe/Gly-Gly-Gly-Arg-Gly-Gly-Gly/Phe is a preferred recognition motif. *Biochemistry* **36**, 5185–5192
37. Cho, E. C., Zheng, S., Munro, S., Liu, G., Carr, S. M., Moehlenbrink, J., Lu, Y. C., Stimson, L., Khan, O., Konietzny, R., McGouran, J., Coutts, A. S., Kessler, B., Kerr, D. J., and Thangue, N. B. (2012) Arginine methylation controls growth regulation by E2F-1. *EMBO J.* **31**, 1785–1797
38. Kaniskan, H. U., Martini, M. L., and Jin, J. (2018) Inhibitors of protein methyltransferases and demethylases. *Chem. Rev.* **118**, 989–1068
39. Ku, N. O., and Omary, M. B. (2000) Keratins turn over by ubiquitination in a phosphorylation-modulated fashion. *J. Cell Biol.* **149**, 547–552
40. Ku, N. O., Lim, J. K., Krams, S. M., Esquivel, C. O., Keeffe, E. B., Wright, T. L., Parry, D. A. D., and Omary, M. B. (2005) Keratins as susceptibility genes for end-stage liver disease. *Gastroenterology* **129**, 885–893
41. Choudhary, C., Weinert, B. T., Nishida, Y., Verdin, E., and Mann, M. (2014) The growing landscape of lysine acetylation links metabolism and cell signalling. *Nat. Rev. Mol. Cell Biol.* **15**, 536–550
42. Haberland, M., Montgomery, R. L., and Olson, E. N. (2009) The many roles of histone deacetylases in development and physiology: implications for disease and therapy. *Nat. Rev. Genet.* **10**, 32–42
43. Outeiro, T. F., Kontopoulos, E., Altmann, S. M., Kufareva, I., Strathearn, K. E., Amore, A. M., Volk, C. B., Maxwell, M. M., Rochet, J. C., McLean, P. J., Young, A. B., Abagyan, R., Feany, M. B., Hyman, B. T., and Kazantsev, A. G. (2007) Sirtuin 2 inhibitors rescue alpha-synuclein-mediated toxicity in models of Parkinson's disease. *Science* **317**, 516–519
44. Guldiken, N., Zhou, Q., Kucukoglu, O., Rehm, M., Levada, K., Gross, A., Kwan, R., James, L. P., Trautwein, C., Omary, M. B., and Strnad, P. (2015) Human keratin 8 variants promote mouse acetaminophen hepatotoxicity coupled with c-jun amino-terminal kinase activation and protein adduct formation. *Hepatology* **62**, 876–886
45. Hu, D., Gur, M., Zhou, Z., Gamper, A., Hung, M. C., Fujita, N., Lan, L., Bahar, I., and Wan, Y. (2015) Interplay between arginine methylation and ubiquitylation regulates KLF4-mediated genome stability and carcinogenesis. *Nat. Commun.* **6**, 8419
46. Chen, W., Daines, M. O., and Hershey, G. K. (2004) Methylation of STAT6 modulates STAT6 phosphorylation, nuclear translocation, and DNA-binding activity. *J. Immunol.* **172**, 6744–6750
47. Harada, M., Strnad, P., Resurreccion, E. Z., Ku, N. O., and Omary, M. B. (2007) Keratin 18 overexpression but not phosphorylation or filament organization blocks mouse Mallory body formation. *Hepatology* **45**, 88–96
48. Strnad, P., Zatloukal, K., Stumptner, C., Kulaksiz, H., and Denk, H. (2008) Mallory-Denk-bodies: lessons from keratin-containing hepatic inclusion bodies. *Biochim. Biophys. Acta* **1782**, 764–774
49. Fickert, P., Trauner, M., Fuchsbichler, A., Stumptner, C., Zatloukal, K., and Denk, H. (2003) Mallory body formation in primary biliary cirrhosis is associated with increased amounts and abnormal phosphorylation and ubiquitination of cytokeratins. *J. Hepatol.* **38**, 387–394
50. Strnad, P., Zhou, Q., Hanada, S., Lazzeroni, L. C., Zhong, B. H., So, P., Davern, T. J., Lee, W. M., and Omary, M. B. (2010) Keratin variants predispose to acute liver failure and adverse outcome: race and ethnic associations. *Gastroenterology* **139**, 828–835, 835.e1–3
51. Zhong, B., Strnad, P., Selmi, C., Invernizzi, P., Tao, G. Z., Caleffi, A., Chen, M., Bianchi, I., Podda, M., Pietrangelo, A., Gershwin, M. E., and Omary, M. B. (2009) Keratin variants are overrepresented in primary biliary cirrhosis and associate with disease severity. *Hepatology* **50**, 546–554

Received for publication February 6, 2018.
Accepted for publication April 15, 2019.